

Incommensurate structure of $\text{InAl}_{1-x}\text{Ti}_x\text{O}_{3+x/2}$ [$x = 0.701(1)$]: comparison between modulated and composite models

P. J. Bereciartua,^{a*} F. J. Zuñiga^a
and T. Brezczewski^b

^aDepartment of Condensed Matter Physics, University of the Basque Country, Aptdo 644, Bilbao, Spain, and ^bDepartment of Applied Physics II, University of the Basque Country, Aptdo 644, Bilbao, Spain

Correspondence e-mail:
pjbereciartu001@ehu.es

Received 22 November 2007

Accepted 28 April 2008

The structure of the monoclinic phase of the compound $\text{InAl}_{1-x}\text{Ti}_x\text{O}_{3+x/2}$ with $x = 0.701(1)$ has been analyzed within the $(3+1)$ -dimensional superspace formalism. Two different models were refined describing the structure as an incommensurate modulated layer and modulated composite, respectively. Both models include the same composition–structure relation. In the composite approach it is derived from the mismatching between the two subsystems. In the incommensurate modulated system, it is derived from a closeness condition between O atomic domains. The distribution and coordination of the cations is discussed and compared with previously proposed models for similar compounds.

1. Introduction

Series of compounds in the systems $\text{In}_2\text{O}_3:\text{TiO}_2:A_2\text{O}_3$, with $A = \text{Al}, \text{Cr}, \text{Mn}, \text{Fe}$ or Ga , and $\text{In}_2\text{O}_3:\text{TiO}_2:BO$, with $B = \text{Mg}, \text{Mn}, \text{Co}, \text{Ni}, \text{Cu}$ or Zn , have been explored (Brown, Flores *et al.*, 1999; Brown, Kimizuka *et al.*, 1999; Brown & Kimizuka, 2001). New phases with flexible compositions have been found within these ternary systems. Single-crystal and powder X-ray diffraction investigations confirmed that these compounds exhibit orthorhombic or monoclinic modifications of the hexagonal InFeO_3 structure (Giaquinta *et al.*, 1994).

The structure consists of layers of edge-sharing InO_6 octahedra alternating with $\text{Fe}-\text{O}$ planes arranged in the shape of honeycombs, as shown in Fig. 1. The deviations of the new compounds from this basic structure depend on their compositions and their synthesis temperatures.

The diffraction patterns of these phases show satellite reflections whose positions change for different compounds. This suggests commensurate and incommensurate modulated structures, depending on the composition. Among the reported phases, the structure and its relationship with composition have been investigated in the solid solution $\text{InFe}_{1-x}\text{Ti}_x\text{O}_{3+x/2}$, with $0.5 \leq x \leq 0.69$ and $0.73 \leq x \leq 0.75$, where the x parameter is fixed by the Fe/Ti ratio. The individual compounds represent points along the $\text{InFeO}_3\text{--In}_2\text{Ti}_2\text{O}_7$ line in the ternary phase diagram of the $\text{In}_2\text{O}_3:\text{TiO}_2:\text{Fe}_2\text{O}_3$ system (Michiue *et al.*, 2000). Their structures can be obtained from the ideal InFeO_3 structure by replacing some Fe atoms in the honeycomb plane with Ti, and including additional O atoms within this plane (hereafter the $M-\text{O}$ plane) to maintain charge neutrality.

The structure of the orthorhombic phase was first reported by Michiue *et al.* (1999) for $\text{InFe}_{1-x}\text{Ti}_x\text{O}_{3+x/2}$ ($x = 2/3$) determined within an average approximation using only main reflections. A single-crystal structural analysis including satellite reflections was later reported by Michiue *et al.* (2001) for the same phase, but a slightly different composition ($x =$

0.61) was considered. They proposed an incommensurate composite structure with two subsystems [superspace group $Cmm(1, 1.305, 0)s00$ and cell parameters $a = 5.835$ (3), $b_1 = 3.349$ (1), $c = 12.082$ (7) and $b_2 = 2.568$ (6) Å, $Z = 4$]. The first subsystem, with periodicity b_1 , consists of InO_6 octahedral layers and Fe/Ti atoms. The second subsystem is composed of the O atoms included in the Fe/Ti–O planes and has a smaller b_2 parameter. The strong displacive modulation of these O atoms gives rise to different environments for the Fe/Ti atoms. If the information of the occupational modulation of the metal atoms is taken into account, it is possible to distinguish a fivefold coordination site, preferably occupied by Fe, and a sixfold coordinated site, occupied by Ti. Besides, this composite model involves a relationship between the composition of the solid solution, given by the parameter x , and the b_1/b_2 mismatch ratio of the two lattices. Since the first subsystem contains two $\text{InFe}_{1-x}\text{Ti}_x\text{O}_2$ per unit cell ($\mathbf{a}, \mathbf{b}_1, \mathbf{c}$) and the second subsystem contains two O atoms per cell ($\mathbf{a}, \mathbf{b}_2, \mathbf{c}$), the charge neutrality leads to the relation $b_1/b_2 = 1 + x/2$, assuming that all positions in the two subsystems are fully occupied. In this case $b_1/b_2 = 1.305$, and therefore $x = 0.61$. This should allow the structure to be predicted for other composition values, at least within the range of the solid solution $0.5 \leq x \leq 0.69$, which corresponds to the orthorhombic phase. Nevertheless, this rule seems to break when approaching the limits of the range. Thus, for $x = 0.533$, the expected $b_1/b_2 = 1.266$ significantly deviates from the reported experimental ratio 1.281 (Michiue *et al.*, 2001). A possible explanation of this might be the existence of vacancies on the metal sites.

Structural studies of the monoclinic phase have been reported for the compounds $\text{InFe}_{1-x}\text{Ti}_x\text{O}_{3+x/2}$ (Michiue *et al.*,

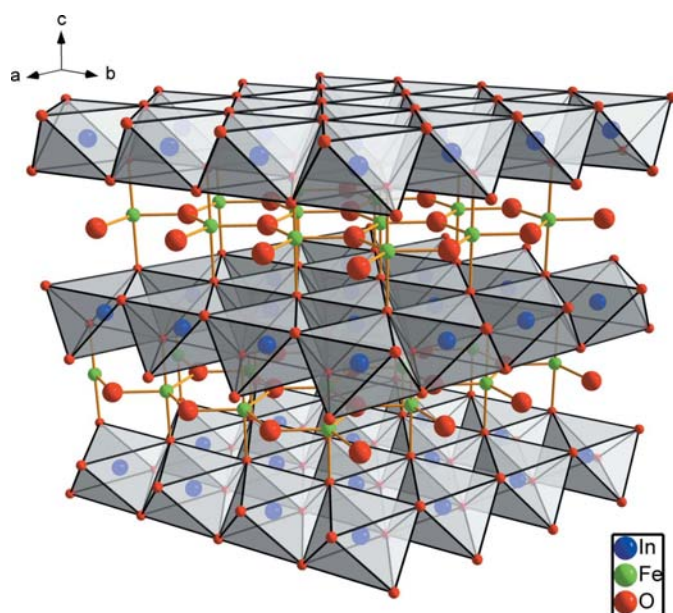


Figure 1

Structure of InFeO_3 . Modifications of this basic structure give rise to the two orthorhombic and monoclinic phases. The structure consists of InO_6 octahedral layers alternating with Fe–O planes along \mathbf{c} .

2002) and $\text{InCr}_{1-x}\text{Ti}_x\text{O}_{3+x/2}$ (Michiue *et al.*, 2004), with $x = 2/3$. In the first case the structure is commensurate with a supercell given by $\mathbf{a}, 3\mathbf{b}_1, \mathbf{c}$. For the second one an incommensurate composite crystal model [superspace group $C2/m(1, 1.345, 0)s0$ and cell parameters $a = 5.9269$ (2), $b_1 = 3.3597$ (1), $c = 6.3583$ (2), $b_2 = 2.4984$ (9) Å and $\beta = 108.09642$ (3)°, $Z = 2$] was refined by the Rietveld method. The structure of this phase is similar to the orthorhombic one, with the alternated stacking of octahedral layers and Cr/Ti–O planes along \mathbf{c} , which is not perpendicular to the layers in this case. Although the b_1/b_2 ratio leads to a composition $x = 0.688$, an ideal value of $x = 2/3$ was fixed for the chemical composition. The discrepancy with the experimental value was assumed to be due to vacancies on the O-atom position. Since the proportion of these vacancies is small, they were not considered in the refinement process.

Li *et al.* (2005) studied the phase relationships of the $\text{In}_2\text{O}_3\text{:TiO}_2\text{:CaO}$ and $\text{In}_2\text{O}_3\text{:TiO}_2\text{:SrO}$ systems. They obtained the phase $\text{In}_6\text{Ti}_6\text{CaO}_{22}$, but the corresponding one for Sr did not appear. They analyzed the structure of the synthesized Ca compound with the Rietveld method. The structural refinement was based on a similar model to that of the Cr compound [superspace group $C2/m(0, 0.389, 0)s0$, $a = 5.951$ (1), $b_1 = 3.422$ (1), $c = 6.352$ (1), $b_2 = 2.464$ (1) Å and $\beta = 108.32$ (1)°, $Z = 2$]. Using the observed modulation wavevector (or the b_1/b_2 ratio), they proposed the composition $\text{In}_6\text{Ti}_{5.93}\text{Ca}_{0.93}\text{O}_{21.79}$ and a structural model with Ca atoms distributed on the octahedral sites and some In atoms in the Ti–O planes. The larger ionic radius of Ca cations explains their preference for the octahedral sites. As in the Fe compound, O atoms in the M –O plane suffer the largest displacive modulation leading to fivefold and sixfold coordination sites for the Ti/In atoms.

In this paper, the structure of the monoclinic phase $\text{InAl}_{1-x}\text{Ti}_x\text{O}_{3+x/2}$ with $x = 0.701$ (1) has been studied with single-crystal X-ray diffraction. Both an incommensurately modulated model and a composite one have been analysed. In the first, a geometrical condition is considered in the superspace structure to avoid O–O distances in the Al/Ti–O plane which are too short (closeness condition). Together with the assumption that all positions are fully occupied, this leads to the structure–composition relationship proposed by Michiue *et al.* (2001), *i.e.* $x = 2(b_1/b_2 - 1) = 2q$, where q is the component of the modulatory wavevector along the unique axis. The composition has been measured with a WDX microprobe. In addition, the cationic distribution and their different coordination environments within the M –O plane have been investigated in detail. Furthermore, the composite description has been compared with the modulated one, concluding that, in fact, they are equivalent models.

2. Experimental

2.1. Synthesis

The synthesis method was analogous to that followed by Brown, Flores *et al.* (1999) for similar systems.

Table 1

Cell parameters of the two studied samples.

The composition is given by $x = 2\left(\frac{b_1}{b_2} - 1\right)$.

	Sample for X-ray single-crystal diffraction experiment	Sample for WDX microanalysis
<i>a</i>	5.857 (4)	5.849 (3)
<i>b</i> (= <i>b</i> ₁)	3.361 (3)	3.358 (1)
<i>c</i>	6.355 (9)	6.348 (3)
β	107.96 (5)	107.86 (5)
<i>q</i>	0.3503 (5)	0.3493 (9)
<i>b</i> ₂	2.489 (2)	2.489 (2)
<i>b</i> ₁ / <i>b</i> ₂	1.3503 (5)	1.3493 (9)
<i>x</i>	0.701 (1)	0.699 (2)

Table 2

Composition measured with the WDX microanalysis.

The resulting values are compared with the starting composition and the atomic percentages obtained within the refined models.

	WDX microanalysis	Starting composition	Modulated model (± 0.1)	Composite model (± 0.1)
In	19.9 (1)	18.75	19.5	19.6
Al	4.8 (2)	6.25	4.7	4.7
Ti	12.6 (2)	12.25	13.1	13.1
O	62.7 (3)	62.5	62.6	62.6

Initial amounts of In₂O₃, TiO₂ and Al₂O₃ were weighed with molar proportions 3:4:1 and carefully mixed together with ethanol in an agate mortar. The resulting mixture was heated to and held at 1373 K for 3 d. This procedure was repeated several times. Each time the sample was weighed and no mass changes were observed. A powder diffractogram was measured and analyzed to confirm the synthesis of the compound.

After this process, the compound was pressed into pellets, heated to 1923 K and slowly cooled in order to improve crystallization. Two single crystals were chosen from the crystallized material. Their lattice parameters were obtained through single-crystal X-ray diffraction. The resulting structural parameters, shown in Table 1, are very similar. Taking into account the structure–composition relationship explained in §1, the two samples are believed to have identical composition. One was employed for the measurement of diffraction intensities, while a wavelength-dispersive X-ray (WDX) microanalysis was performed with the other.

2.2. Microanalysis

The WDX microanalysis was carried out in a scanning electron microscope Jeol JSM 6400, equipped with Jeol spectrometers. The composition was measured at 15 different points of the sample, with nearly constant results. The averaged values of atomic percentages are given in Table 2. They are compared with the values corresponding to the starting composition, and with the percentages obtained taking into account the refined atomic occupancies of the two models.

Table 3

Crystallographic and experimental data.

Crystal data	
Chemical formula	Al _{0.256} In _{1.044} O _{3.350} Ti _{0.700}
<i>M_r</i>	213.89
Cell setting, space group	Monoclinic, <i>C2/m</i> (0, 0.3503, 0) <i>s</i> 0
Superspace group	<i>C2/m</i> (0, 0.3503, 0) <i>s</i> 0
Temperature (K)	293
<i>a</i> , <i>b</i> (= <i>b</i> ₁), <i>c</i> (Å)	5.857 (4), 3.361 (3), 6.355 (5)
β (°)	107.96 (5)
<i>q</i>	0.3503 (5)
<i>b</i> ₂	2.489 (2)
<i>V</i> (Å ³)	119.00 (17)
<i>Z</i>	2
<i>D_x</i> (g cm ⁻³)	5.967
Radiation	Mo <i>K</i> α
μ (mm ⁻¹)	12.360
Crystal form, colour	Plate, colourless
Crystal size (mm)	0.15 × 0.06 × 0.02
Data collection	
Diffractometer	Oxford Diffraction CCD
Data collection method	ω scans
Absorption correction	Numerical
<i>T_{min}</i>	0.31
<i>T_{max}</i>	0.83
No. measured, independent and observed reflections	8896, 1733, 994
Criterion for observed reflections	<i>I</i> > 3 σ (<i>I</i>)
<i>R_{int}</i>	0.045
θ_{\max} (°)	36.6
Refinement	
Refinement on	<i>F</i>
<i>R</i> [<i>F</i> ² > 2 σ (<i>F</i> ²)], <i>wR</i> (<i>F</i> ²), <i>S</i>	0.032, 0.059, 1.49
No. of reflections	1733
No. of parameters	57
Weighting scheme	Based on measured s.u.s. $w = 1/[\sigma^2(F) + 0.0004F^2]$
(Δ/σ) _{max}	0.001
$\Delta\rho_{\max}$, $\Delta\rho_{\min}$ (e Å ⁻³)	2.47, -2.37
Extinction method	B–C type 1 Gaussian isotropic (Becker & Coppens, 1974)
Extinction coefficient	0.00103 (6)

Computer programs used: *CrysAlis CCD* (Oxford Diffraction, 2005), *JANA2000* (Prteicek *et al.*, 2000).

2.3. X-ray data collection

The X-ray single-crystal diffraction experiment was carried out with an Xcalibur four-circle diffractometer equipped with a CCD area detector. The data collected were reduced with the *CrysAlis RED* software package (Oxford Diffraction, 2005).

The main crystallographic and data collection parameters are listed in Table 3.¹

The reconstructed reciprocal space sections allow two interpretations: as an incommensurate modulated structure or as a composite one. Within the first one, two sets of reflections can be identified: main reflections, indexed using a monoclinic cell with parameters *a* = 5.857 (4), *b* = 3.361 (3), *c* = 6.355 (5) Å

¹ Supplementary data for this paper are available from the IUCr electronic archives (Reference: CK5031). Services for accessing these data are described at the back of the journal.

and $\beta = 107.96 (5)^\circ$, and satellite reflections up to third order, related to the former ones through a modulation wavevector $\mathbf{q} = q\mathbf{b}^* = 0.3503 (5)\mathbf{b}^*$.² On this basis the systematic reflection conditions are $hklm$: $h + k = 2n$ and $0k0m$: $m = 2n$. These systematic extinctions and the refinement results indicate that the superspace group of the structure is $C2/m(0, 0.3503, 0)s0$. It can be converted to $B2/m(0, 0, 0.3503)s0$ (No. 12.4 in Janssen *et al.*, 1992) by $\mathbf{a}^* = -\mathbf{a}^*$, $\mathbf{b}^* = \mathbf{c}^*$, $\mathbf{c}^* = \mathbf{b}^*$ and $\mathbf{q}' = q\mathbf{c}^*$. The symmetry operations are $(0, 0, 0, 0; \frac{1}{2}, \frac{1}{2}, 0, 0) + x_1, x_2, x_3, x_4$; $-x_1, x_2, -x_3, \frac{1}{2} + x_4$; $x_1, -x_2, x_3, \frac{1}{2} - x_4$; $-x_1, -x_2, -x_3, -x_4$. The non-centrosymmetric superspace group $C2(0q0)s$ has been considered in the refinement process. However, it was rejected because the rise in the number of parameters did not improve the refinement results significantly.

In the interpretation of composite crystals two monoclinic subsystems have been suggested with the global superspace group $C2/m(0, 0.3503, 0)s0$. The first subsystem has the parameters $a = 5.857 (4)$, $b_1 = 3.361 (3)$, $c = 6.355 (5)$ Å and $\beta = 107.96 (5)^\circ$, while the second one has the same a , c and β parameters, but $b_2 = 2.489 (3)$ Å. The matrices of the two subsystems are

$$W^1 = \begin{pmatrix} 1 & 0 & 0 & 0 \\ 0 & 1 & 0 & 0 \\ 0 & 0 & 1 & 0 \\ 0 & 0 & 0 & 1 \end{pmatrix} \quad W^2 = \begin{pmatrix} 1 & 0 & 0 & 0 \\ 0 & 1 & 0 & 1 \\ 0 & 0 & 1 & 0 \\ 0 & 1 & 0 & 0 \end{pmatrix}. \quad (1)$$

Each subsystem contains specific subsets of main and satellite reflections and there are some reflections which are satellites in both subsystems.

3. Refinement

The program *JANA2000* (Petricek *et al.*, 2000) was used to refine both models.

First, an average structure was refined using only main reflections. The resulting model is very similar to that proposed by Michiue *et al.* (2004) for the system with $x = 0.66$. The average positions of In and M atoms (Al, Ti) are fixed by symmetry, while coordinates of the O atoms were refined. Anisotropic atomic displacement parameters (ADPs) were considered for all atoms. However, as this model does not explain satellite reflections, the average structure is a rough approximation and modulations have to be taken into account.

3.1. Modulated structure

In the starting model, only In and O atoms of the octahedral layers (In1 and O1), and atoms of the M site (Al and Ti with occupancies 1/3 and 2/3, respectively) were included. ADPs were not included during the initial stages to avoid correlations with modulational parameters. At this point, the values of the reliability factors were $R_{\text{obs}} = 0.497$ and $wR_{\text{all}} = 0.729$.

² The modulation wavevector chosen in this work does not resemble that used by Michiue *et al.* (2004), but that reported by Li *et al.* (2005). Thus, the satellite reflections are related to the main reflections in a simpler way.

The positions and the displacive modulations of these atoms were refined, considering three harmonic functions for In, Al and Ti positional modulations, and one for the O atomic domain. As Al and Ti share the same M position, their modulations were restricted to be identical in order to avoid correlations between the corresponding parameters. This modification decreases R factors to $R_{\text{obs}} = 0.120$ and $wR_{\text{all}} = 0.227$.

In the next step a difference-Fourier map was calculated around the average position of the O atom in the M -O plane (O2). The corresponding sections are represented in Fig. 2. The observed residual electronic density has two main characteristics. The first is a residual electron density close to zero for certain values of the internal coordinate x_4 ($0.15 \leq x_4 \leq 0.45$). The other feature is a linear relationship between the internal coordinate x_4 and the displacement modulation along x_2 , which can be seen in Fig. 2(b). Besides, the $x_1 - x_4$ section, represented in Fig. 2(a), showed a sinu-

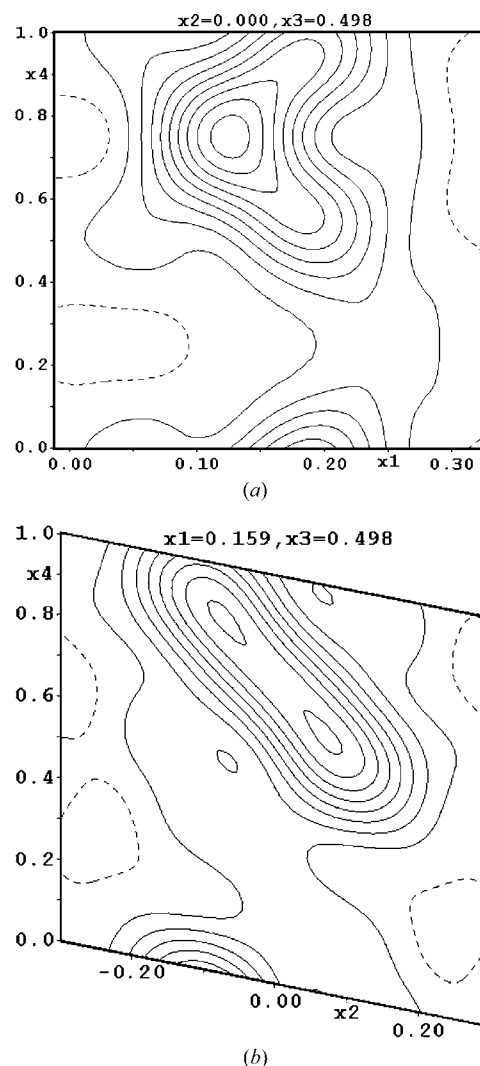


Figure 2 Difference-Fourier maps around the O2 position. The residual electronic density can be modeled by an atomic domain with a displacive modulation which is sinusoidal in the $x_1 - x_4$ plane (a) and linear in the $x_2 - x_4$ plane (b). Contour interval $1 \text{ e } \text{Å}^{-3}$.

soidal modulation. Taking into account all these details, the O2 atomic domain was modelled as a sawtooth function combined with orthogonalized harmonic displacive functions. The sawtooth function represents an atomic domain with the following features. On one hand, it only extends within a certain interval of the internal coordinate x_4 in $[x_4^0 - \frac{\Delta}{2}, x_4^0 + \frac{\Delta}{2}]$ (occupational modulation). On the other hand, it exhibits a linear positional modulation given by $\mathbf{u} = 2\mathbf{u}_0 \frac{x_4 - x_4^0}{\Delta}$ (where x_4^0 , Δ and \mathbf{u}_0 are the centre, the width and the displacement at the extreme of the sawtooth function, respectively). The displacive modulation along x_1 and x_3 can be described by means of orthogonalized harmonic functions which have the same existence range in x_4 as the sawtooth function. Details of these functions and the orthogonalization can be found in the manual of the program *JANA2000* (Petricek *et al.*, 2000). The resulting refined model is shown in Fig. 3. The sawtooth function and the sinusoidal modulation are drawn on the electronic density map. This inclusion of the atomic domain of O2 reduces R factors to $R_{\text{obs}} = 0.075$ and $wR_{\text{all}} = 0.131$.

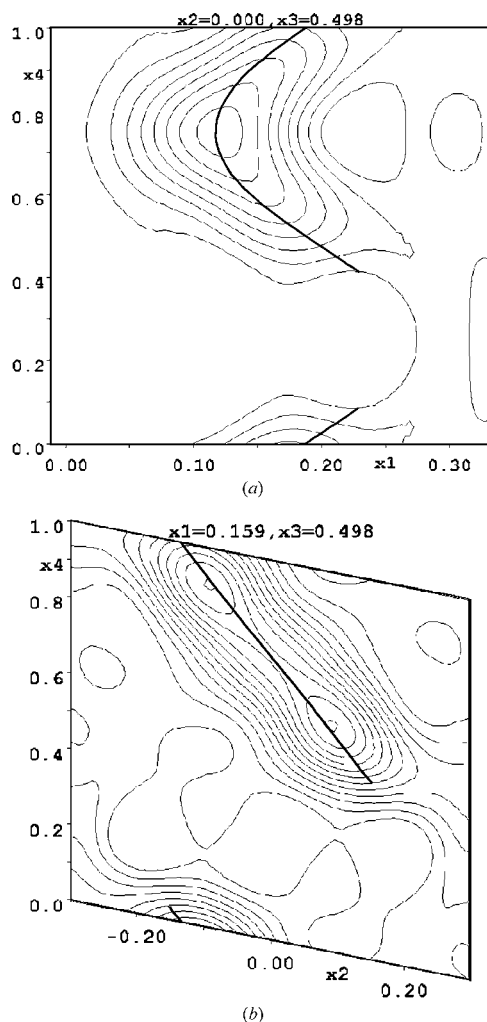


Figure 3
 F_{obs} -Fourier map of the O2 atom within the modulated model. Sections (a) $x_1 - x_4$ and (b) $x_2 - x_4$ show a sinusoidal and linear displacive modulation, respectively. Contour interval $2 \text{ e } \text{Å}^{-3}$ and $1 \text{ e } \text{Å}^{-3}$, respectively.

At this point, attempts to refine the Al and Ti occupation failed because of the strong correlations appearing between the two parameters. Restricting these parameters by means of a charge balance equation did not improve the results, as meaningless negative values were obtained for the Al occupation. Besides, the refinement led to negative values for the ADP of the M site.

These observations point out that a higher number of electrons is necessary to model this site. As the WDX microprobe analysis suggests an excess of In and a deficiency of Al, a small amount of In was included at the M site (In2). The occupational parameters were thus fixed at $\text{Occ}(\text{Al}) = 0.28$, $\text{Occ}(\text{Ti}) = 0.67$ and $\text{Occ}(\text{In2}) = 0.05$.

In subsequent refinement two equations were used to restrict the occupancy parameters. The first is a direct consequence of charge neutrality (assuming that InO_6 octahedral layers are fully occupied)

$$3\text{Occ}(\text{Al}) + 3\text{Occ}(\text{In2}) + 4\text{Occ}(\text{Ti}) = 1 + 4\Delta(\text{O2}). \quad (2)$$

As a second restriction we assumed that the M site in the M -O plane is fully occupied, *i.e.*

$$\text{Occ}(\text{Al}) + \text{Occ}(\text{Ti}) + \text{Occ}(\text{In2}) = 1. \quad (3)$$

This assumption is supported by WDX microprobe results in the following manner. The atomic percentage of Al, as a function of the occupational parameters, is given by

$$\frac{2\text{Occ}(\text{Al})}{2 + 2\text{Occ}(\text{Al}) + 2\text{Occ}(\text{Ti}) + 2\text{Occ}(\text{In2}) + 4 + 4\Delta(\text{O2})} \quad (4)$$

considering full occupancy for the octahedral layers. Analogous expressions are obtained for the Ti and In percentages. Taking into account the sum of the percentages of In, Al and Ti measured in the WDX microprobe (37.3%), the following equation is obtained

$$\frac{2 + 2p}{2p + 6 + 4\Delta(\text{O2})} = 0.373, \quad (5)$$

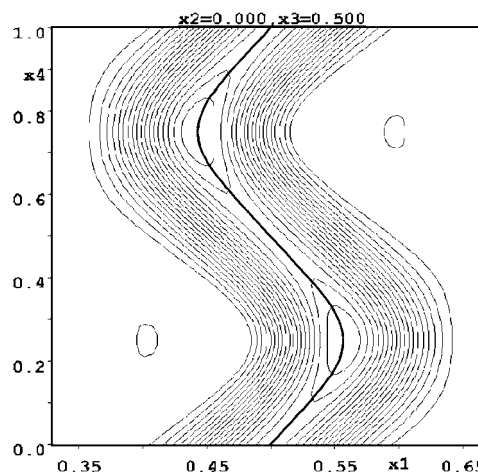


Figure 4
Fourier map of the M position. The variation of the electronic density along the atomic domain is explained by the occupational modulation of this site. Contour interval $5 \text{ e } \text{Å}^{-3}$.

where $p = \text{Occ}(\text{Al}) + \text{Occ}(\text{Ti}) + \text{Occ}(\text{In2})$. Assuming $\Delta(\text{O2}) \simeq 2/3$ leads to $p = 1.02$, from which (3) follows. Restricting the refinement with (2) and (3) avoided the correlations between occupational parameters, and converged to the values $\text{Occ}(\text{Al}) = 0.275$ (10), $\text{Occ}(\text{Ti}) = 0.667$ (7) and $\text{Occ}(\text{In2}) = 0.058$ (12), with $R_{\text{obs}} = 0.074$ and $wR_{\text{all}} = 0.129$.

Once these average occupations were established, a Fourier map around the M site (see Fig. 4) showed a significant variation of the electronic density along the atomic domain. This suggests that not only the position but also the occupation of this site should be modulated.

To start, only occupational modulation for Ti and Al was included, as they represent approximately 95% occupancy in the M site. Moreover, since no vacancies have been considered, the occupational modulation of the two atoms should be complementary. This implies restrictions for the coefficients ($\text{Occ}_n^{\text{sin}}$ and $\text{Occ}_n^{\text{cos}}$) of the harmonic functions describing the occupational modulation of these atoms. Once the occupational modulation for Al and Ti was refined, an occupational modulation for In2 was included in the model. The resulting values for each atom type are plotted in Fig. 5 as functions of t . The result is consistent with the variation of the electronic density along the atomic domain of the M position, as shown by the Fourier map in Fig. 4. Although the general R factors remain almost constant ($R_{\text{obs}} = 0.070$ and $wR_{\text{all}} = 0.104$), there are noticeable changes in the R factors for the second-order satellites (from $R_{\text{obs}}/wR_{\text{all}} = 0.125/0.231$ to $0.107/0.134$) and the third-order satellites (from $R_{\text{obs}}/wR_{\text{all}} = 0.412/0.562$ to $0.213/0.384$).

In the following stage, the occupancy of the O2, given by the width of the sawtooth, was also refined, leading to a value of $\Delta(\text{O2}) = 0.683$ (2). However, an examination of the possible environments of the M site shows that such a width involves unrealistically short O—O distances of around 0.8 Å at certain values of t (as in Fig. 6). In order to avoid this, a closeness condition was included for the sawtooth function of O2. This condition prevents two atomic domains from overlapping by restricting the end of one domain and the beginning of the

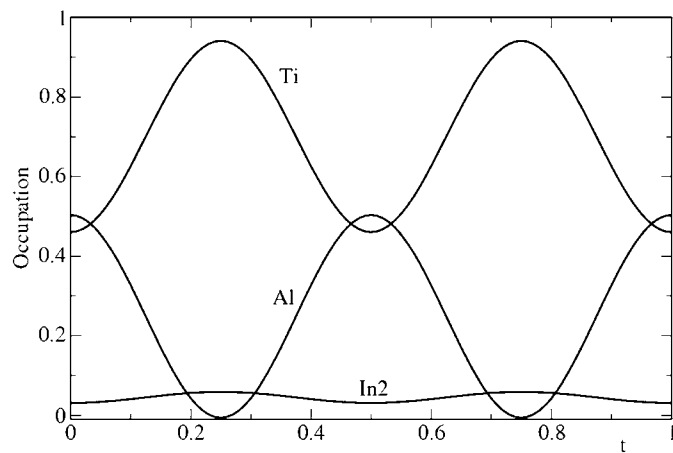


Figure 5
Occupational modulation of the Al, Ti and In2 atoms.

next to the same t value. In Fig. 7 symmetrically related domains of O2 are represented. To avoid their overlap, the width Δ has to fulfil the equation $\Delta(\text{O2}) + [\Delta(\text{O2}) - q] = 1$, as derived from geometrical considerations (see Fig. 7). Therefore, the width of the O2 sawtooth is a function of q , which is the module of the modulational wavevector \mathbf{q}

$$\Delta(\text{O2}) = \frac{1 + q}{2}. \quad (6)$$

As q is experimentally determined, the value of $\Delta(\text{O2})$ was fixed to $\Delta(\text{O2}) = 0.6751$ in the subsequent refinement process. This modification barely changes the R factors ($R_{\text{obs}} = 0.070$ and $wR_{\text{all}} = 0.103$).

In the final stage of the refinement process, anisotropic ADPs were included in the structural model. Up to two harmonics for the ADP modulation of the M site and the In1 of the octahedral layers were included.

Final parameters obtained at the end of the refinement process are shown in Table 4 and the overall agreement factors in Table 5.

3.2. Composite structure

In order to compare the modulated model with some previously proposed structures for compounds isostructural with this monoclinic phase ($\text{InCr}_x\text{Ti}_{1-x}\text{O}_{3+x/2}$, with $x = 2/3$, by Michiue *et al.*, 2004, and $\text{In}_6\text{CaTi}_6\text{In}_{22}$ by Li *et al.*, 2005), we also refined a composite model.

The composite model considers two incommensurate subsystems. As mentioned in §2 a , c and β parameters are common for the two subsystems, while b_1 and b_2 are incommensurate. The first subsystem includes the octahedral layers (In1 and O1) and the metal atoms of the M —O plane (M site,

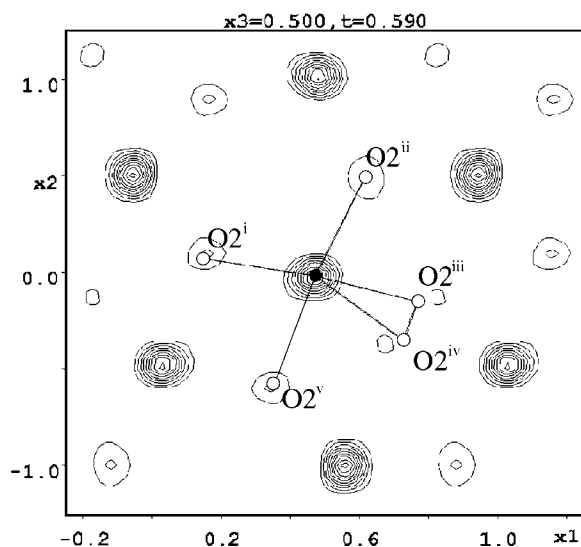


Figure 6
 M -atom environment for $t = 0.59$. The closeness condition avoids this sort of configuration with O—O distances of *ca* 0.8 Å. The central black point represents the M site and the open ones are the O atoms at the M —O plane. Symmetry codes: (i) x_1, x_2, x_3, x_4 ; (ii) $\frac{1}{2} + x_1, \frac{1}{2} + x_2, x_3, x_4$; (iii) $1 - x_1, x_2, 1 - x_3, \frac{1}{2} + x_4$; (iv) $\frac{1}{2} + x_1, -\frac{1}{2} + x_2, x_3, x_4$; (v) $\frac{1}{2} - x_1, -\frac{1}{2} + x_2, 1 - x_3, \frac{1}{2} + x_4$. Contours $10 e \text{ \AA}^{-3}$.

Table 4

Structural parameters of the modulated model.

The coefficients of the corresponding Fourier sum are sorted by terms (s for sine, c for cosine, o for orthogonalized) and n . The occupational modulation parameters for each type of atom in the M site are indicated, if they are different, while the displacive modulation parameters are common for these atoms.

	x	y	z	Occupancy	U_{iso}
In	0	0	0	1	0.00571 (11)
s,1	0.02002 (6)	0	0.00511 (5)	–	–
c,1	0	0	0	–	–
s,2	0	–0.00228 (7)	0	–	–
c,2	0	0	0	–	–
s,3	–0.00006 (5)	0	0†	–	–
c,3	0	0	0	–	–
M	0.5	0	0.5	(Al) 0.256 (8)	0.0100 (3)
–	–	–	–	(Ti) 0.700 (6)	–
–	–	–	–	(In2) 0.044 (10)	–
s,1	0.0545 (2)	0	0.00745 (13)	0	–
c,1	0	0	0	0	–
s,2	0	–0.0261 (2)	0	(Al) 0.256 (8)	–
–	–	–	–	(Ti) –0.242 (9)	–
–	–	–	–	(In2) –0.014 (3)	–
c,2	0	0	0	0	–
s,3	–0.00242 (18)	0	0.00158 (16)	–	–
c,3	0	0	0	–	–
O1	0.3888 (4)	0	0.1709 (4)	1	0.0053 (6)
s,1	0.0285 (4)	0	0.0011 (3)	–	–
c,1	0	0†	0	–	–
O2	0.1597 (4)	0	0.4983 (4)	1	0.0181 (7)
o,1	0.0352 (5)	0	0.0008 (4)	–	–
o,2	0	0.0009 (7)	0	–	–
o,3	0	0.0006 (6)	0	–	–
o,4	0†	0	–0.0036 (4)	–	–
\mathbf{u}_0	0	–0.155 (2)	0	–	–
x_4^0/Δ	0.75/0.6751 (6)	–	–	–	–

† Refined value is not significant.

with Al, Ti and In2). The second subsystem only contains the O atoms of the M –O plane (O2). The matrices relating the two subsystems are given in §2.

The refinement process was similar to that described for the modulated model, using the restrictions (2) and (3) explained in the previous section.

Initially only In1, O1 and M atoms were taken into account, and their positions and displacive modulations were refined. At this point, ADPs were not considered to avoid correlations with the modulation parameters.

A difference-Fourier map around the O2 position showed a discontinuous atomic domain with a sawtooth-like modulation in the $x_2 - x_4$ plane. As before, this domain was described by means of a sawtooth and several orthogonalized harmonic functions. Refining the width of the sawtooth function led to $\Delta(\text{O2}) > 0.5$. This value implies that this atomic domain should overlap with the equivalent atomic domain corresponding to the symmetry operation $-x_1 + \frac{3}{2}, x_2, -x_3 + 1, x_4 + \frac{1}{2}$. This overlap gives rise to O–O distances of ca 0.8 Å. To avoid these distances, the width of the sawtooth was fixed to $\Delta(\text{O2}) = 0.5$. The resulting model is consistent with the electron density obtained in a Fourier map, shown in Fig. 8.

In subsequent refinement stages, the model was completed including the occupational modulation of the M atoms and anisotropic ADPs, modulated for In1 and M atoms.

Table 5

Refinement results for modulated model.

Refinement on	F
$R_{\text{obs}}, wR_{\text{all}}$	
All reflections	0.0322, 0.0602
Main reflections	0.0257, 0.0324
First-order satellites	0.0321, 0.0461
Second-order satellites	0.0623, 0.0939
Third-order satellites	0.2172, 0.3532
G.o.f. (obs/all)	1.58, 1.53
No. of reflections	1733
No. of parameters	57
Weighting scheme	$w = [\sigma^2(F_o) + (0.02 F_o)^2]^{-1}$
$(\Delta/\sigma)_{\text{max}}$	0.001
$\Delta\rho_{\text{max}}, \Delta\rho_{\text{min}}$	2.47, –2.37
Extinction method	B–C type 1 Gaussian isotropic (Becker & Coppens, 1974)
Extinction coefficient	0.00103 (6)

Final parameters and overall agreement factors are shown in Tables 6 and 7, respectively.

4. Discussion

One of the features of the resulting structures in this work (common for the two models) is the distribution of the different cations between two possible positions: the octahedra and the M sites. Centres of the octahedral layers are fully occupied by In atoms, while in the M site there are Al, Ti and In. The amount of In included at the M position (In2) is so small (less than 5%) that it might be considered as uncertain. But this result is unlikely to be an artificial effect of the refinement process since the WDX microprobe analysis

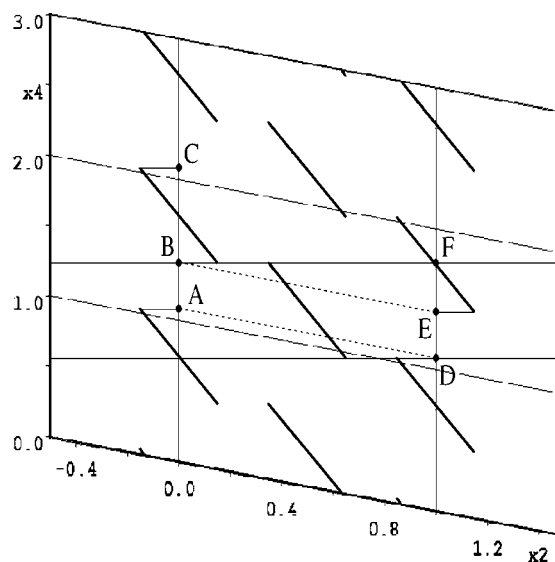


Figure 7

Representation of symmetrically equivalent O2 atomic domains (thick segments). Thin lines perpendicular to the x_4 axis represent different t sections. The closeness condition avoids O–O distances which are too short (see Fig. 6) by imposing the same t value to the ends of two consecutive atomic domains. The two t sections indicated, delimiting an O2 atomic domain, imply that $DF = \Delta(\text{O2})$. Owing to the superspace construction, $EF = q$. Therefore, it can be deduced that $AC = AB + BC = (\Delta(\text{O2}) - q) + \Delta(\text{O2}) = 1$ [see (6)].

Table 6

Structural parameters of the composite model.

The coefficient of the corresponding Fourier sum are sorted by terms (s for sine, c for cosine, o for orthogonalized) and *n*. The occupational modulation parameters for each type of atom in the *M* site are indicated, while the displacive modulation parameters are common for these atoms.

	<i>x</i>	<i>y</i>	<i>z</i>	Occupancy	<i>U</i> _{iso}
In	0	0	0	1	0.00571 (11)
s,1	0	0.2003 (6)	0	0	0.0511 (5)
c,1	0	0	0	–	–
s,2	0	–0.00228 (7)	0	–	–
c,2	0	0	0	–	–
s,3	–0.00017 (5)	0	0†	–	–
c,3	0	0	0	–	–
<i>M</i>	0.5	0	0.5	(Al) 0.255 (8)	0.0100 (3)
–	–	–	–	(Ti) 0.701 (6)	–
–	–	–	–	(In2) 0.044 (10)	–
s,1	0.0545 (2)	0	0.00745 (13)	0	–
c,1	0	0	0	0	–
s,2	0	–0.0261 (2)	0	(Al) 0.255 (8)	–
–	–	–	–	(Ti) –0.241 (9)	–
–	–	–	–	(In2) –0.014 (3)	–
c,2	0	0	0	0	–
s,3	–0.00243 (18)	0	0.00158 (16)	–	–
c,3	0	0	0	–	–
O1	0.3888 (4)	0	0.1709 (5)	1	0.0052 (6)
s,1	0.0285 (4)	0	0.0011 (3)	–	–
c,1	0	0†	0	–	–
O2	0.6597 (4)	0.25	0.4983 (4)	1	0.0181 (8)
o,1	0	0†	0	–	–
o,2	0.0353 (5)	0	0.0010 (4)	–	–
o,3	0	0†	0	–	–
o,4	0.0014 (5)	0	–0.0035 (4)	–	–
u ₀	0	–0.126 (4)	0	–	–
<i>x</i> ₄ ⁰ /Δ	0.5/0.5	–	–	–	–

† Refined value is not significant.

supports the result. Moreover, the inclusion of In2 allows the occupational parameters and the ADPs of the atoms at the *M* site to be refined. Otherwise, the refinement process leads to chemically meaningless values for the Al and Ti occupations and their ADPs become negative. A similar amount of In included at the *M* site was proposed by Michiue *et al.* (2000) within the average structure of the compound InTi_{0.75}Fe_{0.25}O_{3.375}. However, three types of atoms sharing the *M* site are not considered in any previous incommensurate models proposed for analogous systems. In the monoclinic phase of the system InCr_{1–*x*}Ti_{*x*}O_{3+*x*/2} with *x* = 2/3 (Michiue *et al.*, 2004), the centres of the octahedral layers are also fully occupied by In cations, but the *M* site includes Cr and Ti cations, in a 1:2 ratio, with no In cations at this position. For the Ti₆In₆CaO₂₂ system (Li *et al.*, 2005), a different distribution is proposed: Ca cations share the octahedral sites with In cations, while the *M* site is occupied by Ti and the remaining In.

Considering the cationic distribution obtained from the refinement process, the composition of the studied system is In_{1+δ}Al_{1–*x*–δ}Ti_{*x*}O_{3+*x*/2} with *x* = 0.701 (1) and δ = 0.045 (10).

It should also be mentioned that the atomic domain of O2 in the composite model is described with a sawtooth function. This is a different result with respect to the composite models previously proposed for this monoclinic phase (Michiue *et al.*, 2001, 2004; Li *et al.*, 2005), where this atomic domain was

Table 7

Refinement results for composite model.

Refinement on	<i>F</i>
<i>R</i> (obs), <i>wR</i> (all)	
All reflections	0.032, 0.060
Reflections subst. 1	0.022, 0.028
Reflections subst. 2	0.033, 0.056
Common reflections	0.039, 0.049
No. of reflections	1733
No. of parameters	57
G.o.f. (obs/all)	1.59, 1.53
Weighting scheme	$w = [\sigma^2(F_o) + (0.02 F_o)^2]^{-1}$
(Δ/σ) _{max}	< 0.0001
Δρ (max/min)	2.47/–2.36
Extinction method	B-C type 1 Gaussian isotropic (Becker & Coppens, 1974)
Extinction coefficient	0.00100 (6)

modelled by means of a truncated sum of harmonic functions. However, a discontinuous modulation function seems more suitable for the electronic density obtained in this work, as can be seen in Fig. 8.

The displacive modulations of all atoms are plotted in Fig. 9 for the modulated model, and in Fig. 10 for the composite one. The positions of the atoms within the octahedral layers (In1 and O1) barely change, while the larger displacements correspond to the O2 atoms in the two models. This strong positional modulation of the O2 atoms along **a** and **b** gives rise to different environments for the *M* atoms in the *M*–O plane.

The *M*–O distances vary from 1.86 to 2.42 Å, as can be seen in the corresponding *t* plot (Fig. 11). They are comparable to the distances obtained from statistical studies by Shannon (1976): Al–O = 1.935, Ti–O = 1.985 and In–O = 2.20 Å. This distribution of the *M*–O distances is very similar to those obtained within the previously proposed models for analogous systems, the orthorhombic phase of the Fe

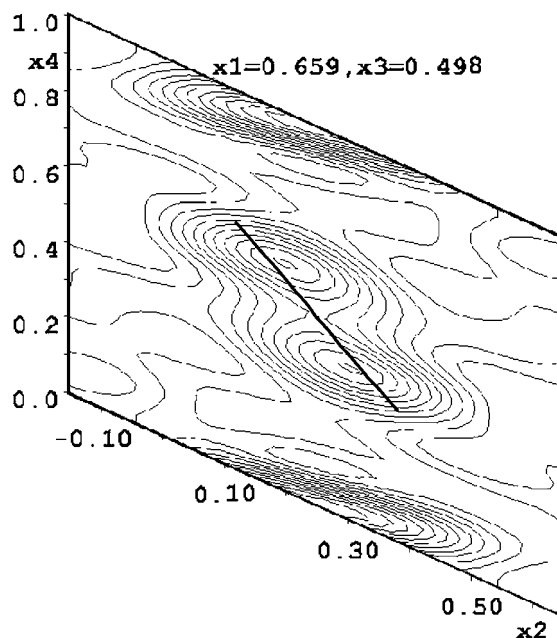


Figure 8 Fourier map of the O2 atom within the composite model. The positional modulation is described by a sawtooth function; contour interval 2 e^{–3}.

compound (Michiue *et al.*, 2001), and the monoclinic phase of the Cr compound (Michiue *et al.*, 2004) and the Ca compound (Li *et al.*, 2005). Moreover, this t plot shows the different environments of the cations in the M –O plane. For some t regions (around $t = 0$ and 0.5) there are six O atoms surrounding the M site with similar distances. These M sites present clearly an octahedral environment, as can be seen in Fig. 12(a). However, for the remaining M sites this environment is distorted, with five O atoms around the cation plus an additional O atom with a larger M –O distance. The maximum distortion occurs at $t = 0.25$ and 0.75, which could be considered to be a fivefold coordination site, as shown in Fig. 12(b).

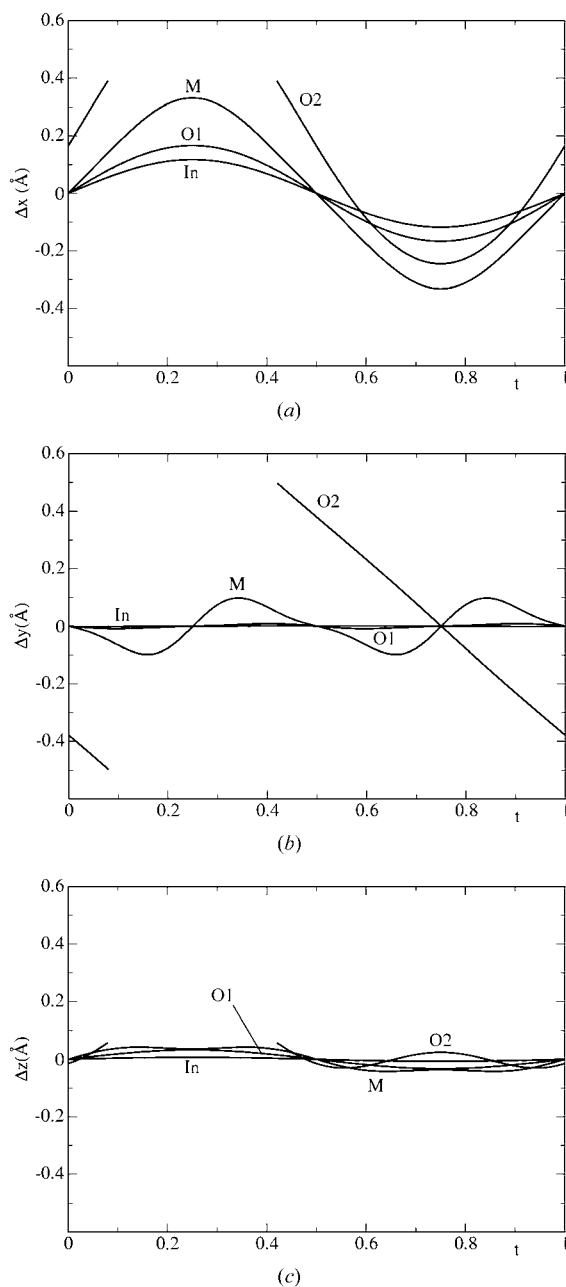


Figure 9
Displacive modulations along x , y and z coordinates of the atoms in the modulated model. Octahedral layers present a smooth modulation, while the largest displacements correspond to O2 atoms in the M –O plane.

Thus, a definite determination of the coordination number is not possible for many M sites.

The interatomic O2–O2 distances within the M –O plane also vary with a minimum value of 2.35 Å, as can be seen in Fig. 13. This shortest O–O distance is similar to that obtained within the previous models; 2.31 Å for the orthorhombic phase of the Fe compound (Michiue *et al.*, 2001) and 2.35 Å for the monoclinic phase of the Ca compound (Li *et al.*, 2005).

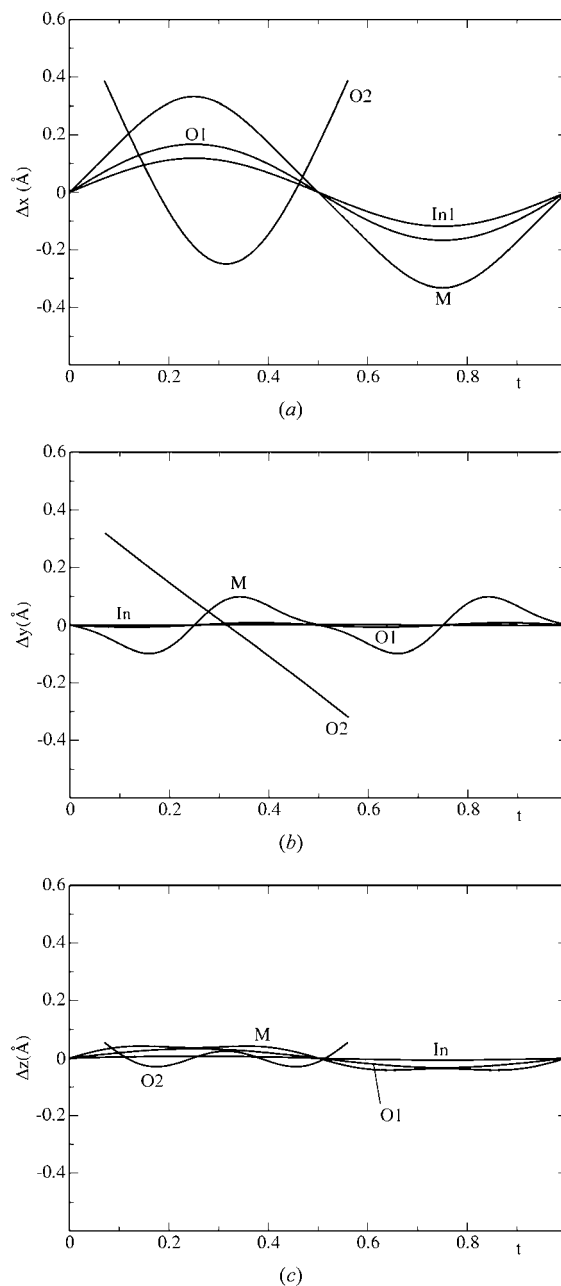


Figure 10
Displacive modulations along x , y and z coordinates in the composite model. The O2 positional modulation is the largest one, as in the modulated model. The O2 atom in the composite model does not correspond to the O2 atom in the modulated model. They are symmetrically equivalent, with $\Delta t = 1/2$ between them, as can be seen in Figs. 9 and 10.

The other O—O distances in the model are larger. Thus, the minimum distances for O2—O1 and O1—O1 are 2.64 and 2.71 Å, respectively.

The reconstruction of the *M*—O plane (see Fig. 14) shows the almost distorted environment that the *M* site exhibits within the range determined by the two limiting environments: octahedra and trigonal bipyramids (including the O atoms of the octahedral layers). Comparing the obtained occupational modulations for the Al, Ti and In2 atoms (see Fig. 5) with the *M*—O distances (Fig. 11), it can be seen that the maxima of the Ti occupation ($t = 0.25$ and 0.75) correspond with environments more similar to fivefold coordination, while the maxima of the Al occupation ($t = 0$ and 0.5) appear at sixfold coordination. In fact, this occupational modulation of the monoclinic phase is opposite that proposed for the orthorhombic phase in the system $\text{InFe}_{1-x}\text{Ti}_x\text{O}_{3+x/2}$ with $x = 2/3$ (Michiue *et al.*, 2001), in which the maxima of the Ti occupational modulation are related to sixfold coordination, while the maximum occupation for the Al corresponds to fivefold coordination. Moreover, this almost trigonal bipyramidal coordination for the Ti atoms could seem doubtful, since an octahedral coordination would be more suitable for them, as in the orthorhombic phase. However, this fivefold coordination for Ti^{4+} cations has also been reported for some similar compounds, like In_2TiO_5 or $\text{Rb}_5\text{Sb}_7\text{TiO}_{22}$. In In_2TiO_5 the Ti cation presents a fivefold coordination, firstly reported as a trigonal bipyramid by Senegas *et al.* (1975). A more accurate structural determination carried out by Gaewdang *et al.* (1993) showed that this fivefold coordination should be better described as a distorted square-based pyramid. In $\text{Rb}_5\text{Sb}_7\text{TiO}_{22}$ (Almgren *et al.*, 1998) Ti and Sb cations share a site with a trigonal bipyramidal coordination. Thus, although not very usual the obtained fivefold coordination for the Ti cations is acceptable.

As an additional result, the bond-valence sum has been calculated for the *M* site. As this position includes several

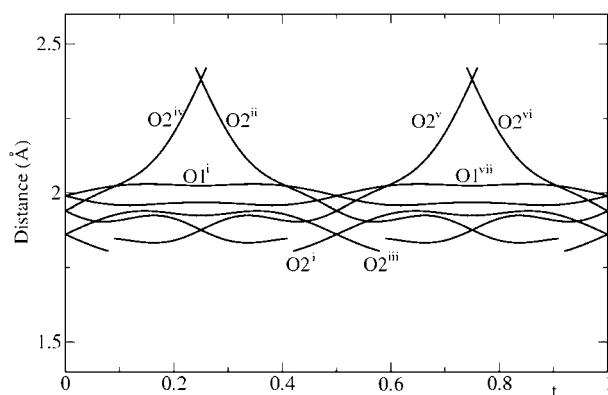


Figure 11
Variation of the distances between *M* and O as function of *t*. It shows sixfold environments at $t = 0$ and 0.5 , and fivefold ones at $t = 0.25$ and 0.75 . Symmetry codes: (i) x_1, x_2, x_3, x_4 ; (ii) $\frac{1}{2} + x_1, \frac{1}{2} + x_2, x_3, x_4$; (iii) $1 - x_1, x_2, 1 - x_3, \frac{1}{2} + x_4$; (iv) $\frac{1}{2} + x_1, -\frac{1}{2} + x_2, x_3, x_4$; (v) $\frac{1}{2} - x_1, -\frac{1}{2} + x_2, 1 - x_3, \frac{1}{2} + x_4$; (vi) $\frac{1}{2} - x_1, \frac{1}{2} - x_2, 1 - x_3, -x_4$; (vii) $1 - x_1, -x_2, 1 - x_3, -x_4$

atoms with different occupational ratios, a special bond-valence parameter has been considered. It is calculated taking into account the different occupations: $R(M) = \text{Occ}(\text{Al})R(\text{Al}) + \text{Occ}(\text{Ti})R(\text{Ti}) + \text{Occ}(\text{In})R(\text{In})$, with $R(\text{Al}) = 1.62 \text{ \AA}$, $R(\text{Ti}) = 1.815 \text{ \AA}$ and $R(\text{In}2) = 1.902 \text{ \AA}$. The bond-valence sum obtained is plotted as a function of *t* in Fig. 15. It agrees with the occupational modulation obtained in the refinement process (Fig. 5), since its value is close to 4 in *t* regions, where Ti nearly fully occupies the *M* site, and is close to 3.5 at *t* regions with similar Al and Ti ratios. This bond-valence sum thus supports the previously discussed conclusion that the *M* sites which are close to fivefold coordination are preferentially occupied by Ti cations.

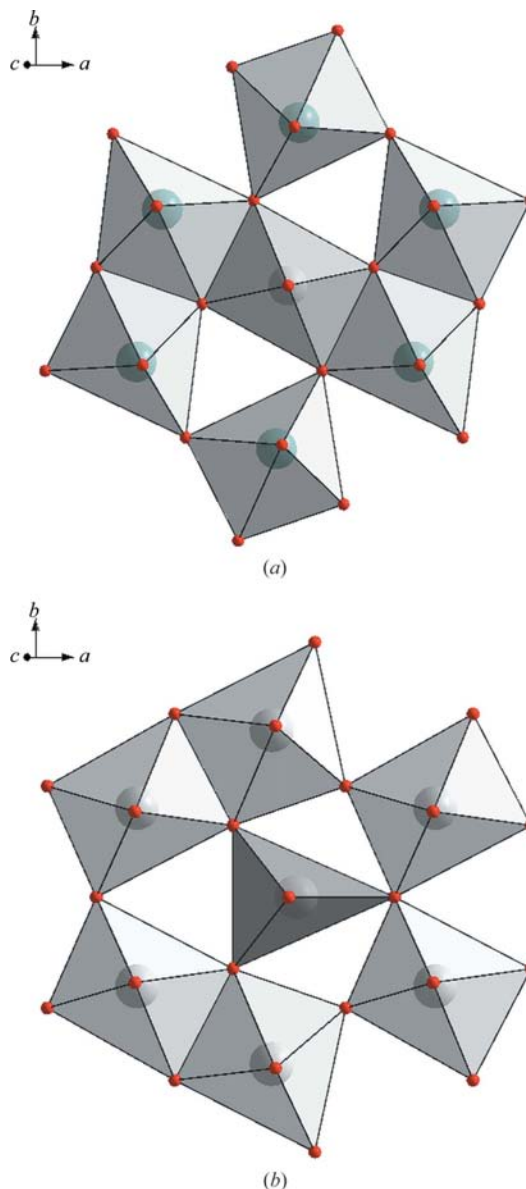


Figure 12
Limiting coordination polyhedra of the *M* site. For $t = 0$ and 0.5 , the *M* site presents an octahedral coordination (a), while the coordination polyhedron corresponding to $t = 0.25$ and 0.75 is a trigonal bipyramid (b). For the rest of the *t* values, the environment of the *M* site is an intermediate distortion between the two of these limiting configurations.

The closeness condition introduced to refine the modulated model must also be commented. It is included to avoid too short O—O distances, as shown in Fig. 6, but at the same time it restricts the composition. Taking into account the final composition, (2) can be rewritten as

$$3(1 - x - \delta) + 3\delta + 4x = 1 + 4\Delta, \quad (7)$$

which leads to $x = 4\Delta - 2$ and, using (6)

$$x = 2q. \quad (8)$$

Besides, as (6) fixes the value of $\Delta(\text{O2})$ to 0.6751, the approximation of $\Delta(\text{O2}) \simeq 2/3$, considered in (5), is valid. In fact, the final value leads to $p = 1.01$.

Equation (8) is equal to that obtained for the composite model based on the incommensurability of the two subsystems. It is noticeable that the role of the closeness condition is

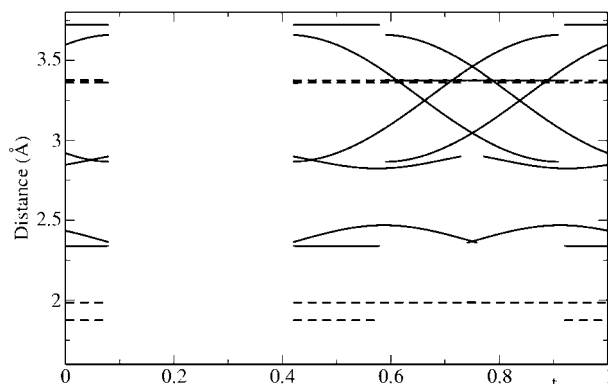


Figure 13
O2—O2 distances as a function of t . The continuous lines represent the distances in the modulated model, while the dashed lines correspond to the average model.

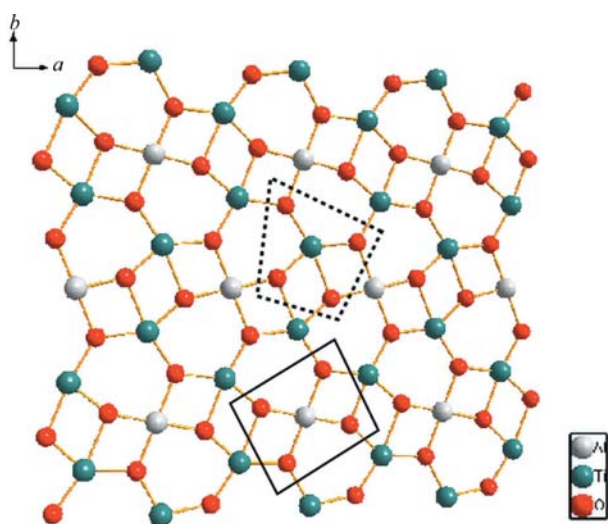


Figure 14
 M —O plane reconstruction. The same figure is obtained for the modulated and the composite model. The different environments for the M site are shown, considering the apical O1 atoms: a distorted square for almost trigonal bipyramids and a square for octahedra. For the M site, the atom with the largest occupation is indicated.

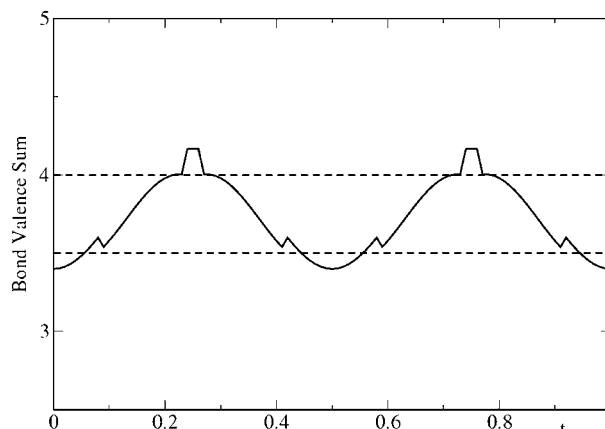


Figure 15
Bond-valence sum for the M site. It is consistent with the refined occupational modulation.

fundamental to obtain (8). Thus, this closeness condition makes it possible to compare the composite model previously proposed for similar systems ($\text{InFe}_{1-x}\text{Ti}_x\text{O}_{3+x/2}$ with $x = 0.61$; Michiue *et al.*, 2001; $\text{InCr}_{1-x}\text{Ti}_x\text{O}_{3+x/2}$ with $x = 0.66$; Michiue *et al.*, 2004; $\text{In}_6\text{Ti}_6\text{CaO}_{22}$; Li *et al.*, 2005) with the modulated model proposed in this work.

The concept of the closeness condition was first introduced by Elcoro *et al.* (2003) to describe the structure of series of the composition $A_{1+x}A'_xB_{1-x}\text{O}_3$. Another example is the pyrrhotite system (Fe_{1-x}S with $0.05 \leq x \leq 0.125$; Izaola *et al.*, 2007). All these models include discontinuous atomic domains which are related as previously explained; the end of an atomic domain and the beginning of a neighbour domain are fixed to the same t value. This restriction implies a condition on the existence range in the x_4 coordinate of these atomic domains, that is there is a relationship between the closeness condition and the flexible composition of the system.

The structural parameters for the two proposed models are listed in Tables 4 and 6. Only the coefficients related to the orthogonalized harmonic functions of the O2 atomic domain are different. However, it is in fact the same atomic domain described in two different superspace groups. This can be checked taking into account the central point (\mathbf{x}_c) and the ends of the atomic domains ($\mathbf{x}_1, \mathbf{x}_2$) in the modulated model: $\mathbf{x}_c = (0.118, 0, 0.502, 0.75)$; $\mathbf{x}_1 = (0.230, 0.151, 0.509, 0.465)$; $\mathbf{x}_2 = (0.230, -0.151, 0.509, 1.035)$. They can be transformed, according to the W^2 matrix, to: $\mathbf{x}'_c = (0.118, 0.75, 0.502, 0)$; $\mathbf{x}'_1 = (0.230, 0.616, 0.509, 0.151)$; $\mathbf{x}'_2 = (0.230, 0.883, 0.508, -0.151)$, which are almost identical to the values: $\mathbf{x}''_c = (0.117, 0.75, 0.502, 0)$; $\mathbf{x}''_1 = (0.230, 0.619, 0.508, 0.153)$; $\mathbf{x}''_2 = (0.230, 0.881, 0.508, -0.153)$ in the composite description. Thus, the two models can be considered to be equivalent descriptions of the same structure.

The authors are grateful to M. L. No and S. Fernández for carrying out the microanalysis experiment, to N. Kimizuka and Y. Michiue for their helpful discussions, and to K. Friese and

G. Madariaga for correcting the manuscript. PJB also thanks Basque Government for financial support. This work was financed by project FIS 2005-04476.

References

- Almgren, J., Svensson, G. & Albertsson, J. (1998). *Acta Cryst.* **C54**, 1206–1209.
- Becker, P. J. & Coppens, P. (1974). *Acta Cryst.* **A30**, 129–147.
- Brown, F., Flores, M. J. R., Kimizuka, N., Michiue, Y., Onoda, M., Mohri, T., Nakamura, M. & Ishizawa, N. (1999). *J. Solid State Chem.* **144**, 91–99.
- Brown, F. & Kimizuka, N. (2001). *J. Solid State Chem.* **157**, 13–22.
- Brown, F., Kimizuka, N., Michiue, Y., Mohri, T., Nakamura, M., Orita, M. & Morita, K. (1999). *J. Solid State Chem.* **147**, 438–449.
- Elcoro, L., Perez-Mato, J. M., Darriet, J. & El Abed, A. (2003). *Acta Cryst.* **B59**, 217–233.
- Gaewdang, T., Chaminade, J., Gravereau, P., García, A., Fouassier, C., Hagenmuller, P. & Mahiou, R. (1993). *Mater. Res. Bull.* **28**, 1051–1060.
- Giaquinta, D. M., Davis, W. M. & zur Loye, H.-C. (1994). *Acta Cryst.* **C50**, 5–7.
- Izaola, Z., González, S., Elcoro, L., Perez-Mato, J. M., Madariaga, G. & García, A. (2007). *Acta Cryst.* **B63**, 693–702.
- Janssen, T., Janner, A., Looijenga-Vos, A. & de Wolff, P. (1992). *International Tables for Crystallography*, Vol. C, pp. 797–844. Dordrecht: Kluwer Academic Publishers.
- Li, Z., Sun, J. L., You, L. P., Jiao, H., Li, G. B., Jing, X. P., Liao, F. H. & Lin, J. H. (2005). *Chem. Mater.* **17**, 2186–2192.
- Michiue, Y., Brown, F., Kimizuka, N., Onoda, M., Nakamura, M., Watanabe, M., Orita, M. & Ohta, H. (2000). *Chem. Mater.* **12**, 2244–2249.
- Michiue, Y., Brown, F., Kimizuka, N., Watanabe, M., Orita, M. & Ohta, H. (1999). *Acta Cryst.* **C55**, 1755–1757.
- Michiue, Y., Onoda, M., Brown, F. & Kimizuka, N. (2004). *J. Solid State Chem.* **177**, 2644–2648.
- Michiue, Y., Onoda, M., Watanabe, A., Watanabe, M., Brown, F. & Kimizuka, N. (2002). *J. Solid State Chem.* **163**, 455–458.
- Michiue, Y., Onoda, M., Watanabe, M., Brown, F. & Kimizuka, N. (2001). *Acta Cryst.* **B57**, 458–465.
- Oxford Diffraction (2005). *Xcalibur CCD CrysAlis*, Version 1.171.28c. Oxford Diffraction Ltd, Abingdon, Oxfordshire, England.
- Petricek, V., Dusek, M. & Palatinus, L. (2000). *JANA2000*. Institute of Physics, Praha, Czech Republic.
- Senegas, J., Manaud, J. P. & Galy, J. (1975). *Acta Cryst.* **B31**, 1614–1618.
- Shannon, R. D. (1976). *Acta Cryst.* **A32**, 751–767.